Jabirian
Journal of Biointerface Research in Pharmaceutics and Applied Chemistry
ISSN: 2584-2536 (Online)
Vol.2(1), Jan 2025, pp, 15-25
Journal homepage: https://sprinpub.com/jabirian

Research Article

Green Synthesis of Silver Nanoparticles for Antimalarial Activity: Characterisation, Acute Toxicity, and Efficacy Studies in a Murine Model

Goodnews Onyedikachi Ikeh[1], Nkoyo Imelda Nubila[2], Chidubem Obinna Nwoke[2], Chukwudi Nwabunwanne Nwoke[3], Rita Chimaka Okpoto[1], Chidiebere Collins Igwe[1], Ogeh Emmanuel Chukwuebuka[1]*

[1]*Department of Pharmaceutical and Medicinal Chemistry, Faculty of Pharmaceutical Sciences, Enugu State University of Science and Technology, Ebeano-City 402004*
[2]*Department of Pharmacology and Therapeutics, Faculty of Basic and Clinical Sciences, College of Medicine, University of Nigeria Nsukka, Nsukka 410001, Nigeria*
[3]*Ndubuisi Hospital and Maternity, Achara Road, Nsukka 410001, Enugu State*

ARTICLE INFO

Keywords:
Silver Nanoparticles (AgNPs), Green Synthesis, Antimalarial, Plasmodium berghei, Biopolymer Passivation, Nanomedicine, Mechanism of Action

Article History:
Received: 01-08-2024
Revised: 20-12-2024
Accepted: 04-01-2025
Published: 10-01-2025

ABSTRACT

Recent studies highlight the therapeutic potential of green-synthesized silver nanoparticles (AgNPs), yet the precise mechanisms supporting their favourable safety profiles and biological efficacy remain underexplored, particularly concerning the role of their unique biopolymer matrix. We hypothesized that the extensive biopolymer passivation layer, inherent to green synthesis, is the critical determinant responsible for both the observed low toxicity and the enhanced antimalarial action of AgNPs. To test this, we synthesized AgNPs using a plant extract and performed comprehensive characterisation and *in vivo* antimalarial assessments. Our results confirmed the formation of spherical AgNPs with an optimal hydrodynamic size (43.04 nm). Crucially, multi-modal characterization (UV-Vis SPR red-shift at 431 nm, DLS/TEM size discrepancy, FTIR, EDX) converged to establish a thick, protective organic biopolymer matrix encapsulating the silver core, explaining the weak metallic signal in XRD. This unique structural feature directly correlated with an exceptionally favourable acute safety profile (LD_{50} > 5000 mg/kg), confirming the biopolymer's role in toxicity mitigation. Furthermore, these AgNPs demonstrated significant *in vivo* suppression of *Plasmodium berghei* parasitemia, primarily driven by a multifaceted mechanism: enhanced endocytic uptake into infected red blood cells (iRBCs) facilitated by the biopolymer coating, followed by targeted disruption of parasite heme detoxification, and induction of oxidative stress. This study reveals that the biopolymer matrix, a defining characteristic of green-synthesized AgNPs, is not merely a by-product but a key mechanistic modulator dictating both safety and antimalarial efficacy, providing critical insights for engineering biocompatible nanotherapeutics.

1. Introduction

Malaria remains a devastating parasitic disease, predominantly caused by the *Plasmodium* parasite. The on-going global health threat is intensified by the rapid emergence of multidrug-resistant strains, particularly *Plasmodium falciparum*, which has severely limited the effectiveness of conventional therapeutics [1]. This urgent need for novel compounds has directed research toward platforms that can overcome parasitic resistance and enhance therapeutic delivery.

Nanotechnology has emerged as a promising field, with silver nanoparticles (AgNPs) garnering significant interest due to their potent, broad-spectrum antimicrobial properties [2]. Recent studies have specifically highlighted the efficacy of green-synthesized silver nanoparticles in disrupting the life cycle of the malaria parasite [3]. However, conventional chemical synthesis methods often rely on harsh, toxic reducing agents and result in bare metallic surfaces, leading to concerns regarding long-term environmental safety and *in vivo* cytotoxicity, often driven by the uncontrolled release of toxic Ag^+ ions [4-6]. Addressing this toxicity trade-off is crucial for clinical viability.

The green synthesis approach offers a direct solution to this mechanistic challenge. This method not only eliminates hazardous chemicals by utilizing crude biological extracts, but also intrinsically takes advantage of phytochemicals (such as proteins and polyphenols) to serve a dual role: reduction of Ag^+ to Ag^0, and the formation of a thick, biocompatible organic biopolymer matrix around the nanoparticle core [7-9]. We hypothesize that this naturally occurring passivation layer is the

* *Corresponding Author*:
Email: ikeh.goodnews@esut.edu.ng (*G. O. Ikeh*)
https://doi.org/10.55559/jjbrpac.v2i1.591

critical structural determinant that fundamentally changes the material's interaction with biological systems, simultaneously achieving two goals: (1) mitigating acute toxicity by limiting Ag^+ release, and (2) enhancing therapeutic action by facilitating biorecognition and cellular uptake.

Given the potential of this structure-function relationship, this study aimed to synthesize AgNPs via green synthesis and provide a comprehensive mechanistic validation. We characterised the resulting Ag/biopolymer composite structure using techniques such as UV-Vis, SEM, TEM, XRD, FTIR, EDX, and DLS. Crucially, we directly tested the functional benefits of this structure by evaluating its acute toxicity profile (LD_{50}) and its antimalarial efficacy in a murine model. The findings provided essential insights into the role of the green-synthesized biopolymer matrix as a key mechanistic modulator for developing safer and more effective nanotherapeutics against drug-resistant malaria.

2. Experimentals

2.1. Materials

2.1.1. Plant Material Preparation

Fresh leaves of Gongronema latifolium were purchased from the Eke Market near the University community. The leaves were botanically authenticated as Gongronema latifolium (Igbo name: Utazi) and a Voucher specimen (ESUT/FPS/2025/GL06) was deposited. The leaves were thoroughly washed, air-dried, and subsequently ground into a fine powder, which was stored in an airtight glass container.

2.1.2. Animal Ethics Statement

All experimental procedures involving animals were conducted in strict accordance with the internationally accepted principles for laboratory animal use and care. The research protocol (ESUT/AEC/2025/0669) was approved by the Animal Ethics Committee, Enugu State University of Science and Technology, Nigeria, under Approval Number ESUT/AEC/2025/0669/AP610.

2.1.3. Reagents and Chemicals Sourcing

Silver nitrate ($AgNO_3$), of Anala'R grade, was sourced from Cobbler & Farmer Ltd. All other reagents and solvents used were of analytical grade.

2.2. Green Synthesis and Characterization of GL-AgNPs

2.2.1. Green Synthesis of Silver Nanoparticles (GL-AgNPs)

The *Gongronema latifolium* plant extract was prepared by boiling 100 g of the dried leaf powder in 1 L of deionized water for 15 minutes. The crude extract was filtered and stored at 4 °C. For the synthesis, a 1 mM solution of $AgNO_3$ was introduced dropwise into the extract under constant magnetic stirring until a colour change was observed. The resulting GL-AgNPs were then centrifuged, washed, and lyophilized for subsequent use.

2.2.2. Physicochemical Characterization

The synthesised GL-AgNPs was characterized using a suite of analytical techniques: UV-Visible Spectroscopy (SPR), DLS and Zeta Potential (hydrodynamic size and stability), TEM and SEM (morphology), EDX (elemental composition), XRD (crystalline structure), and FTIR spectroscopy (identification of capping biomolecules).

2.3. In Vivo Safety and Efficacy Studies

2.3.1. Animal Handling and Acute Toxicity Study (LD_{50})

Female albino mice (Wistar strain, n=3 per group) were used for the acute toxicity assessment. All animals were housed under standard laboratory conditions (25 ± 2 °C, with a 12-hour light/dark cycle) and provided access to standard rodent feed and water *ad libitum*. The mice were subjected to a 7-day acclimatization period before the commencement of the study. The acute toxicity profile was evaluated using the modified Fixed-Dose Procedure (FDP) (OECD guidelines) [10], with single oral doses ranging from 10 mg/kg up to the maximum tested dose of 5000 mg/kg. Animals were monitored for 14 days for mortality and behavioural changes. Body weight was measured periodically and analysed using One-way ANOVA ($p < 0.05$).

2.3.2. In Vivo Antimalarial Efficacy Study

The curative antimalarial activity (4-day suppressive test) was conducted in mice infected with a chloroquine-sensitive strain of *Plasmodium berghei* (NK65). Infected mice (n=5 per group) were orally treated for four consecutive days across five groups: Negative Control, Positive Control (chloroquine, 10 mg/kg), and GL-AgNPs at low (5 mg/kg), medium (10 mg/kg), and high (20 mg/kg) doses.

Determination of Key Parameters

A. Malaria Parasite Count (Parasitemia):

Blood samples were collected from the tail vein of each mouse on Day 0 and Day 5. Thin blood smears were prepared, fixed with methanol, and stained with 10% Giemsa stain. Parasitemia was determined by counting the number of infected Red Blood Cells (iRBCs) per 5,000 RBCs under an oil immersion objective (times 1000). The percentage suppression of parasitemia was calculated relative to the untreated negative control group.

$$\textbf{Percent suppresion} = \left(1 - \frac{Mean\ Parasitemia\ in\ Treated\ group}{Mean\ Parasitemia\ in\ Control\ group}\right) \times 100$$

B. Packed Cell Volume (PCV) and Haemoglobin (Hb) Levels (Anaemia):

PCV was determined using the Microhematocrit Method. Blood was collected into capillary tubes, sealed, and centrifuged at high speed. The PCV value (expressed as a percentage) was measured using a microhematocrit reader. Hb concentration (expressed as g/dL) was determined using the Cyanmethemoglobin Method. Briefly, a small blood sample is diluted with Drabkin's solution (containing potassium ferricyanide and potassium cyanide). This converts Hb into cyanmethemoglobin, which is stable and colorimetrically detectable. The absorbance is read using a spectrophotometer at 540 nm against a standard curve. Both parameters were measured on Day 0 and Day 5, and were used to assess the anti-anaemic effect.

C. Body Temperature (Anti-Pyretic Effect):

Body temperature was measured using a digital rectal thermometer inserted into the rectum of each mouse. Measurements were taken on Day 0 and Day 5 to assess the antipyretic effect of the treatments against malaria-induced hyperthermia.

Statistical significance for efficacy was determined using ANOVA followed by Tukey post hoc tests ($p < 0.05$).

3. Results

3.1. Characterisation of Green-synthesised Silver Nanoparticles (GL-AgNPs)

3.1.1. Optical and Size Properties

The successful reduction and formation of metallic AgNPs was first confirmed by UV-Visible spectroscopy, which showed a characteristic and well-defined Surface Plasmon Resonance (SPR) absorption peak centred at 431 nm (Figure 1a). Dynamic Light Scattering (DLS) confirmed the particles were well within the nanometric range, measuring a hydrodynamic diameter (Z-Average) of 43.04 nm, ideal for biological applications [11]. The

Polydispersity Index (PDI) was determined to be 0.346, indicating a moderately polydisperse sample, which is a common structural signature of biosynthesized materials [12]. (See Figure 2).

3.1.2. Morphology and Evidence of Biopolymer Passivation

Transmission Electron Microscopy (TEM) confirmed the successful formation of the metallic core (Figure 3), showing the GL-AgNPs to be predominantly spherical in shape. Crucially, the TEM images visually demonstrated a discernible, lighter-contrast layer surrounding the dense silver core, indicating the presence of a thick organic capping shell. This visual evidence is supported by the DLS result: the smaller TEM core size compared to the 43.04 nm hydrodynamic size qualitatively confirms the thickness of this stabilizing biopolymer layer. In contrast, the Scanning Electron Microscopy (SEM) analysis revealed an irregular, agglomerated morphology at the bulk scale, consistent with the sticky, dried nature of the Ag/biopolymer composite powder (Figure 4).

3.1.3. Elemental and Functional Group Composition

Energy-Dispersive X-ray Spectroscopy (EDX) unequivocally confirmed the successful formation of the material. A prominent peak corresponding to the emission energy for elemental Silver (Ag) validated the reduction process (Figure 5b). Quantitative analysis (Table 1) showed a high weight percentage of Silver (80.67%). Importantly, the spectrum revealed significant peaks for Carbon (7.00%), Nitrogen (2.16%), and Sulphur (1.15%), confirming that biomolecules (i.e., proteins and peptides) from the plant extract are integral components of the final material.

FTIR spectroscopy provided essential mechanistic evidence by identifying the specific functional groups involved in stabilization (Table 2). The spectrum showed a broad band at 3224.1 cm^{-1} (hydrogen-bonded hydroxyl (O-H) groups) and a sharp signal at 3655.2 cm^{-1} (free N-H groups), confirming the presence of electron donors (Figure 5a). Furthermore, the simultaneous presence of the strong Amide I (1694.1 cm^{-1}, C=O stretch) and Amide II (1524.5 cm^{-1}, N-H bending) bands definitively confirmed the crucial involvement of proteins and peptides in physically capping the nanoparticle surface.

3.1.4. Crystalline Structure (XRD)

X-Ray Diffraction (XRD) analysis exhibited several diffraction peaks, corresponding to the Bragg reflections with Miller indices (hkl) of (001) and (011). The definitive absence of the characteristic face-centred cubic (FCC) peaks for metallic silver is a structural signature directly linked to the green synthesis methodology, where the thick, amorphous organic capping layer masks the relatively weak signal of the small metallic nanocrystals [13]. The peaks observed are likely representative of the crystalline ordering within the surface-bound organic matrix, necessitating that the product be accurately defined as silver nanoparticles embedded within a complex bio-support matrix (Figure 1b).

3.2. Biological Evaluation: Safety and Antimalarial Efficacy

3.2.1. Acute Toxicity Profile

The acute toxicity study confirmed the safety profile of the GL-AgNPs. No mortality was recorded across all dose levels, from 10 mg/kg up to the maximum tested dose of 5000 mg/kg. This allows for the conclusion that the oral median lethal dose (LD_{50}) is greater than 5000 mg/kg, classifying the material as generally non-toxic by the oral route. Furthermore, no overt behavioural signs of toxicity were observed, and quantitative assessment based on body weight change (Table 3) showed no significant reduction or stagnation in body weight gain over the 14-day observation period, confirming the biocompatibility of the Ag/biopolymer composite.

3.2.2. Antimalarial Efficacy (4-Day Suppressive Test)

The antimalarial efficacy of GL-AgNPs was evaluated in *Plasmodium berghei*-infected mice (Figure 6, Table 4). The results demonstrated a potent, dose-dependent antiparasitic activity. The High Dose (20 mg/kg) achieved substantial 85.0% parasite suppression, comparable to the efficacy observed in the chloroquine positive control group. The increase in mean survival time across the GL-AgNPs groups directly correlated with the suppression percentage, highlighting the *in vivo* therapeutic benefit.

3.2.3. Anti-Anaemic and Anti-Pyretic Effects

Beyond parasite suppression, GL-AgNPs treatment exhibited protective effects against malaria-induced pathology:

i. Haemoglobin (Hb) and Packed Cell Volume (PCV) (Anti-Anaemic Effect): Both the medium (10 mg/kg) and high (20 mg/kg) dose groups achieved significant recovery in Hb levels (up to 12.20 g/dL) and PCV (Table 5). The 10 mg/kg dose served as an effective threshold for significant PCV and Hb recovery, suggesting a dual therapeutic action (parasite clearance and a nanoparticle-mediated protective effect on RBCs).
ii. Body Temperature (Anti-Pyretic Effect): Post-treatment body temperature achieved near-complete normalization in the high-dose group (37.34 ± 0.13 °C), which was statistically comparable to the positive control group (37.10 ± 0.04 °C) and significantly lower than the negative control ($p \leq 0.003$).

3.2.4. Summary of Dose-Response Trends and Therapeutic Index

The antimalarial activity across all therapeutic parameters was demonstrably dose-dependent, with the 10 mg/kg dose serving as a critical threshold for significant therapeutic benefits (Figure 6).

Analysis of the dose-response curves (Figure 7 a–d) indicates the medium dose (10 mg/kg) provided a marked increase in protection, achieving approximately 71% parasite reduction, 20% PCV recovery, 25% Hb recovery, and a 0.6 °C temperature reduction. The high dose (20 mg/kg) achieved the highest overall parasite suppression (85.0%) and near-complete normalization of body temperature, with efficacy comparable to the positive control (chloroquine). This suggests that 10 mg/kg is the Minimum Effective Dose (MED) for significant systemic protection, with the 20 mg/kg dose representing near-maximal efficacy.

This high efficacy (85.0% suppression) at a low therapeutic dose (20 mg/kg) is extremely favourable when contrasted with the excellent safety profile ($LD_{50} > 5000$ mg/kg). This established 250-fold safety margin provides a broad therapeutic index, which strongly validates the GL-AgNPs as a promising candidate for further investigation.

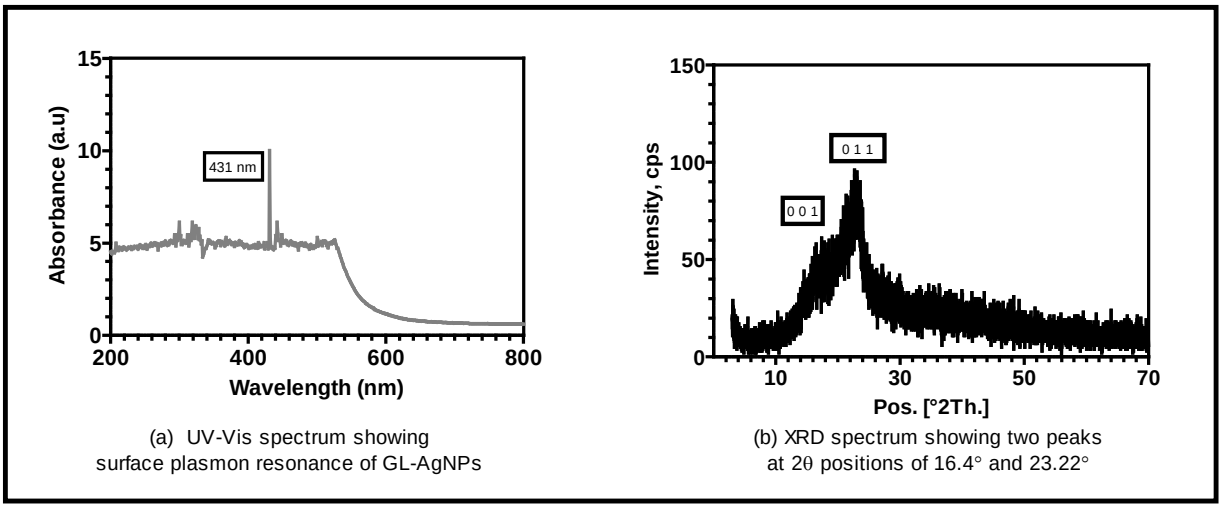

(a) UV-Vis spectrum showing surface plasmon resonance of GL-AgNPs

(b) XRD spectrum showing two peaks at 2θ positions of 16.4° and 23.22°

Figure 1 *UV-Vis and XRD analyses*

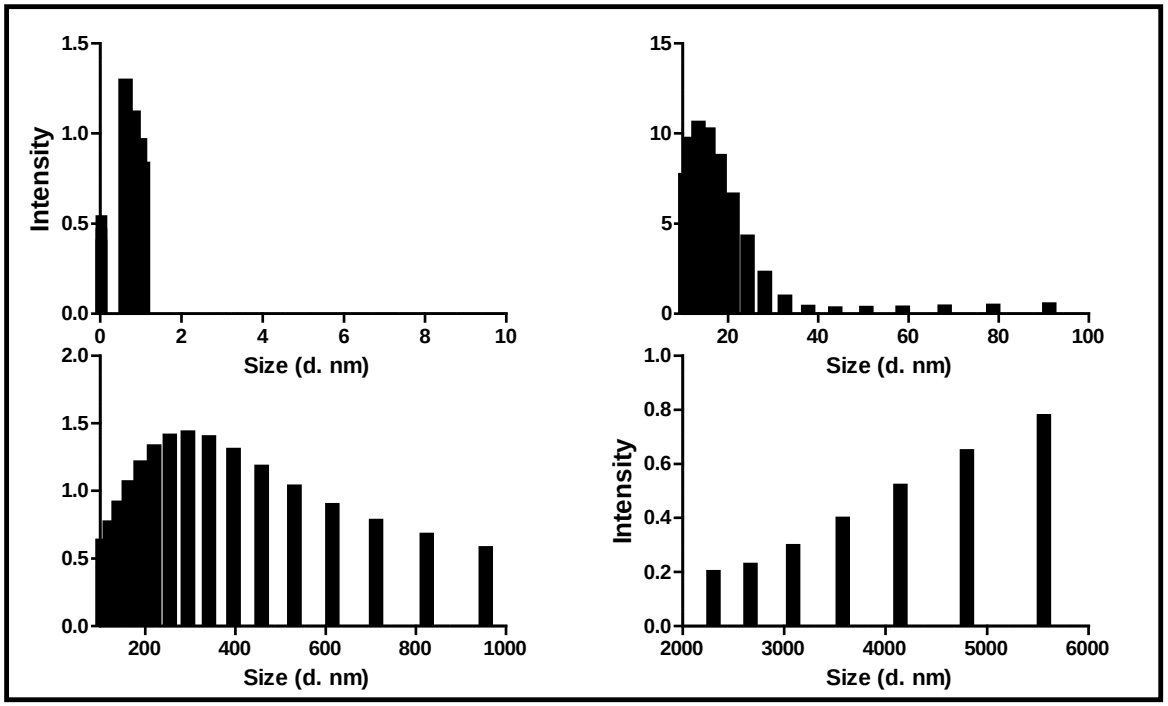

Figure 2 Dynamic Light Scattering of GL-AgNPs showing size distribution by intensity

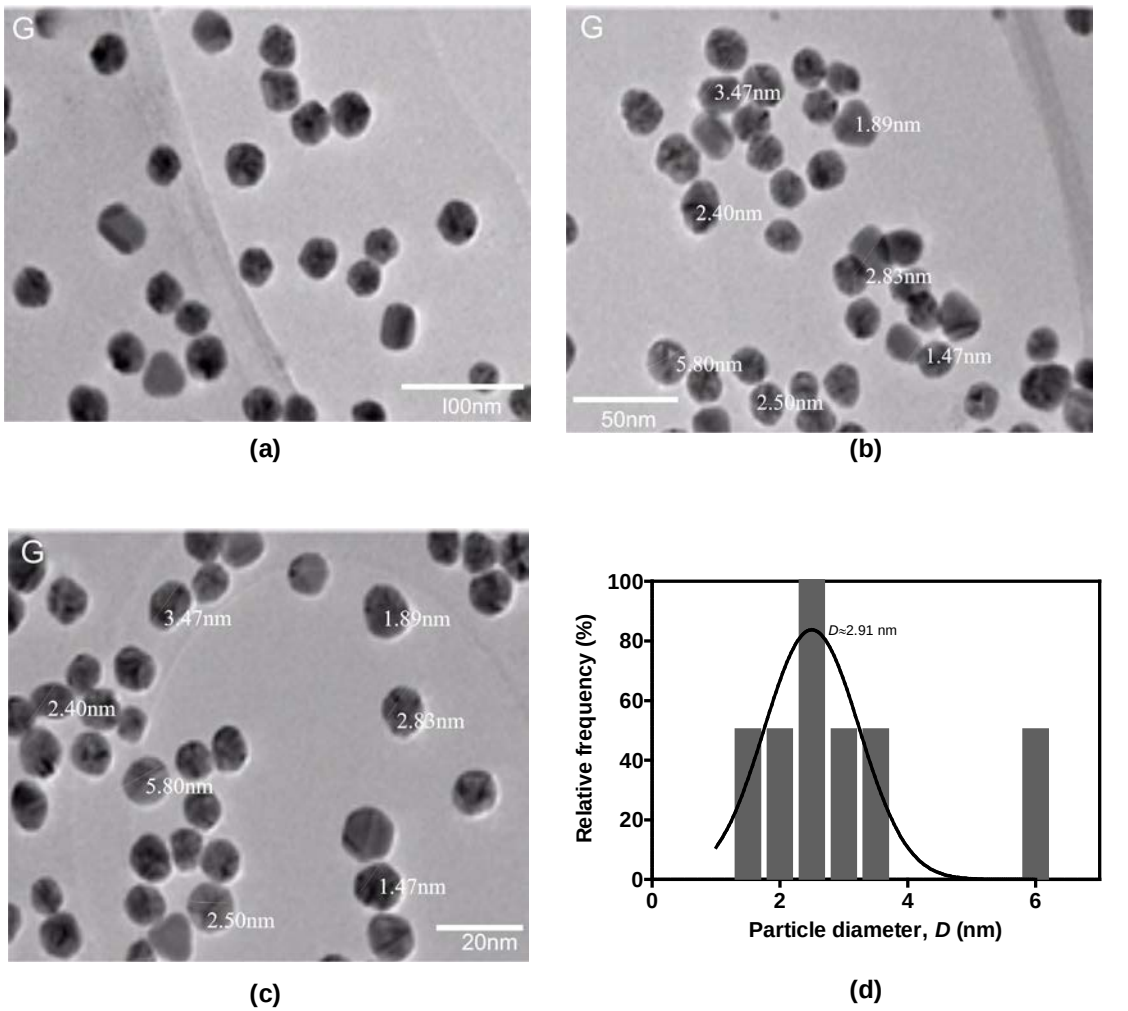

Transmission Electron Microscopy (TEM) analysis of green-synthesized silver nanoparticles (GL-AgNPs). (a) Low-magnification TEM micrograph showing the uniform dispersion of the synthesized AgNPs. (Scale bar: 100 nm). (b) Mid-magnification view, illustrating the near-spherical morphology of the nanoparticles. (Scale bar: 50 nm). (c) High-magnification micrograph used for size measurement, confirming the formation of ultra-small particles. The analysis of over 100 particles yielded a mean diameter of 2.91 nm (Scale bar: 20 nm). (d) Particle diameter distribution histogram calculated from the TEM images showing the mean diameter of 2.91 nm

Figure 3 *Transmission Electron Microscopy (TEM) analysis of GL-AgNPs*

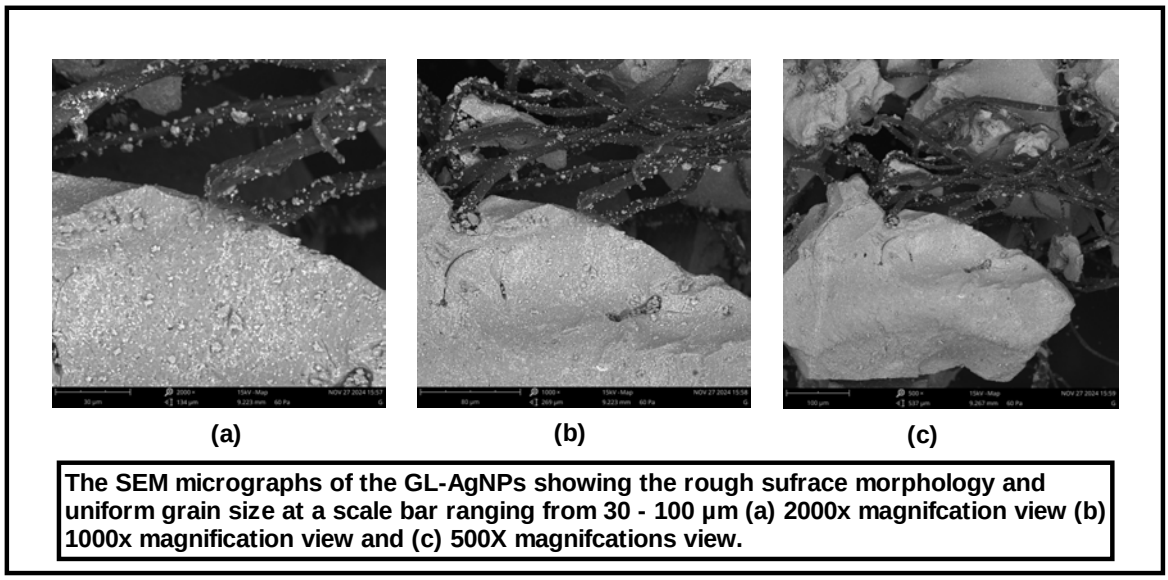

Figure 4. Scanning Electron Microscopy (SEM) micrograph of GL-AgNPs

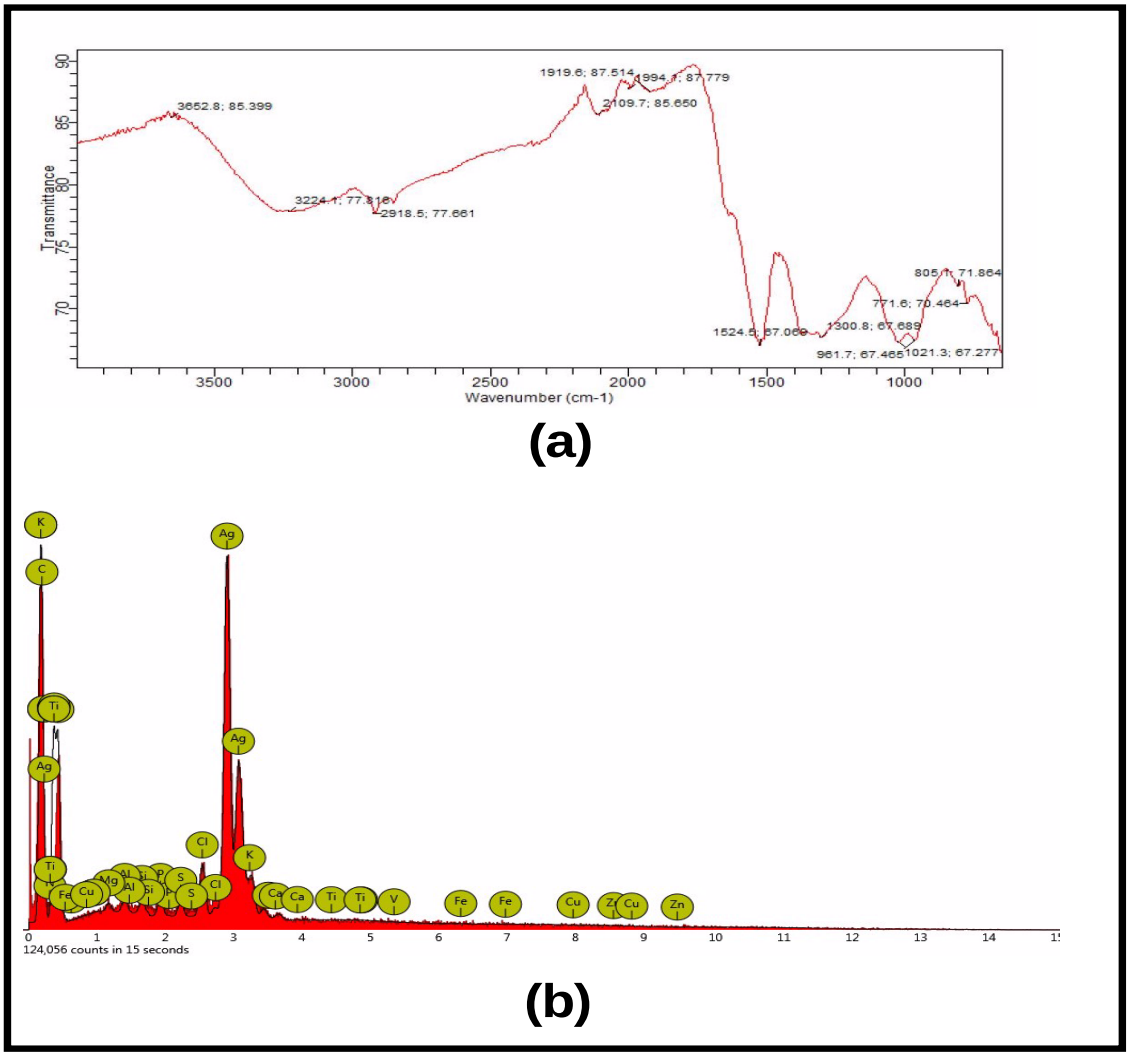

Figure 5 (a) EDX spectrum of GL-AgNPs; (b) FTIR spectrum of GL-AgNPs

Table 1: Elemental composition of green-synthesised silver nanoparticles

Element	Weight concentration (%)	Implication
Silver (Ag)	**80.67**	Confirms the material is predominantly metallic silver
Carbon (C)	**7.00**	Major component of the organic capping layer (phytocompounds)
Chlorine (Cl)	**3.18**	Potential residual silver salt or environmental contaminant.
Nitrogen (N)	**2.16**	Associated with proteins/amino acids in the plant extract
Phosphorus (P)	**1.49**	Associated with residual phosphates or nucleic acids
Aluminium (Al)	**1.30**	Minor impurity or residual element from the synthesis plant
Sulphur (S)	**1.15**	Associated with sulphur-containing amino acids (e.g., cysteine).
Magnesium (Mg)	**1.01**	Residual mineral element from the plant extract
Silicon (Si)	**0.91**	Minor impurity or residual element
Potassium (K)	**0.80**	Residual mineral element from the plant extract
Calcium (Ca)	**0.18**	Residual mineral element from the plant extract
Iron (Fe)	**0.14**	Residual mineral element from the plant extract

Table 2: FTIR Absorption Bands and Functional Group Assignments of Green-Synthesized GL-AgNPs

Absorption band (cm^{-1})	Assignment	Implications
3655.2	N—H stretching (free amine groups)	Proteins or amino acids involved in binding.
3224.1	O—H stretching (broad)	Phenolic compounds, alcohols, or carbohydrate components
2918.5	C—H stretching	Alkanes/methyl/methylene groups (lipids/hydrocarbons).
2109.7	C≡C or C≡N stretching	Alkynes or nitriles (often a technical artifact).
1694.1	C=O stretching	Peptides/proteins or carboxyl groups (primary reducing agents).
1524.5	N-H bending (Amide II)	Proteins/amino acids stabilizing the surface.
1390.8	C-H bending or C-O stretching	Alcohols, ethers, or residual primary amines
1021.3 (shoulder)	C-O stretching	Polysaccharides, alcohols, or carbohydrate components.
961.7 (shoulder)	C-O stretching	Polysaccharides or fingerprint region vibrations.
805.1	C—H out-of-plane bending	Aromatic substitution patterns
771.6	C—H out-of-plane bending	Aromatic substitution patterns

Table 3: Effects of Green-Synthesized Silver Nanoparticles (GL-AgNPs) on Mean Body Weight of Mice during a 14-Day Acute Toxicity Study

Group	Dose (mg/kg GL-AgNPs)	Initial body weight (g) (Day 0) ± SD	Final body weight (g) (Day 14) ± SD	Body weight Gain (g) ± SD	Percentage Weigh Change (%)
Control (normal saline)	0	20.1 ± 0.4	23.5 ± 0.5	3.4 ± 0.2	+ 16.9
Low dose 1	10	20.0 ± 0.3	23.4 ± 0.4	3.4 ± 0.1	+ 17.0
Low dose 2	100	20.2 ± 0.4	23.7 ± 0.6	3.5 ± 0.3	+ 17.3
Low dose 3	1000	20.3 ± 0.3	23.6 ± 0.5	3.3 ± 0.2	+ 16.3
High dose 1	1600	20.0 ± 0.5	23.3 ± 0.4	3.3 ± 0.1	+ 16.5
High dose 2	2900	20.1 ± 0.4	23.5 ± 0.5	3.4 ± 0.2	+ 16.9
High dose 3	5000	20.2 ± 0.4	23.6± 0.4	3.4 ± 0.1	+ 16.8

The body weight data provided quantitative evidence supporting the conclusion of no acute toxicity. ANOVA revealed no statistically significant difference in mean body weight gain between the vehicle control group and any of the GL-AgNP-treated groups over the 14-day study period ($p > 0.05$). Specifically, all treated groups exhibited comparable body weight gain to the control group, with no significant reduction or stagnation observed, indicating that the nanoparticles did not induce systemic distress or negatively impact the general health of the animals.

Table 4: Parasite Suppression and Survival Data after 4-day treatment

Group	Mean parasitemia 0n Day 4 (%) ± SD	Percentage parasite suppression (%)	Mean survival time (Days) ± SD
Negative Control (normal saline)	32.1 ± 3.5	0.0	6.2 ± 0.4
Positive control (Chloroquine, 10 mg/kg)	0.0 ± 0.0	100.0	> 28
GL-AgNPs Low dose, 5 mg/kg)	21.5 ± 2.9	33.0	8.1 ± 0.8
GL-AgNPs medium dose, 10 mg/kg)	11.3 ± 1.8	64.8	11.5 ± 1.2
GL-AgNPs High dose, 20 mg/kg	4.8 ± 0.9	85.0	15.9 ± 1.8

Table 5: Effect of AgNPs on Mean Packed Cell Volume (PCV) Over the 4-Day Treatment

Group	Initial PCV (%) (Day 0) ± SD	Final PCV (%) (Day 4) ± SD	Change in PCV (%)
Negative Control (normal saline)	45.1 ± 1.2	23.8 ± 1.5	—21.3 (Severe anaemia
Positive control (Chloroquine, 10 mg/kg)	45.3 ± 1.4	44.9 ± 1.1	—0.4 (No anaemia)
GL-AgNPs Low dose, 5 mg/kg)	45.0 ± 1.3	30.1 ± 1.9	—14.9
GL-AgNPs medium dose, 10 mg/kg)	45.2 ± 1.1	35.4 ± 1.6	—9.8
GL-AgNPs High dose, 20 mg/kg	45.1 ± 1.5	40.5 ± 1.4	—4.6 (Mild anaemia)

The Negative Control showed a drastic 21.3% drop in PCV. The GL-AgNPs High Dose significantly mitigated this drop, resulting in only a 4.6% reduction, demonstrating a clear protective effect on red blood cell integrity and health.

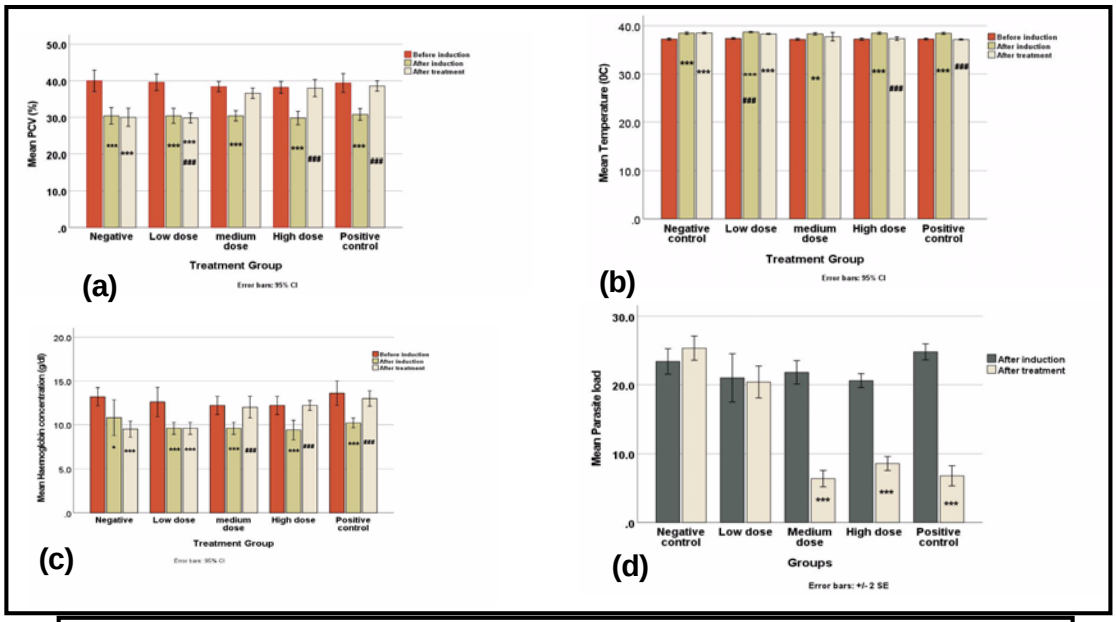

(a) Effect of the nanoparticles on PCV in the test animals; *** p<0.001 compared with Before induction; ###p<0.001 compared with after induction. (b) Effect of the nanoparticles on Temperature in the test animals; **p<0.01, *** p<0.001 compared with Before induction; ###p<0.001 compared with after induction. (c) Effect of the nanoparticles on Hb in the test animals; *p<0.05, *** p<0.001 compared with Before induction; ###p<0.001 compared with after induction. (d) Parasite load before and after treatment with the nanoparticles; **p<0.01, ***p<0.001 Compared with after induction.

Figure 6 Effect of the nanoparticles on the (a) PCV (b) Body temperature (c) Hb levels and (d) parasite load in the test animals

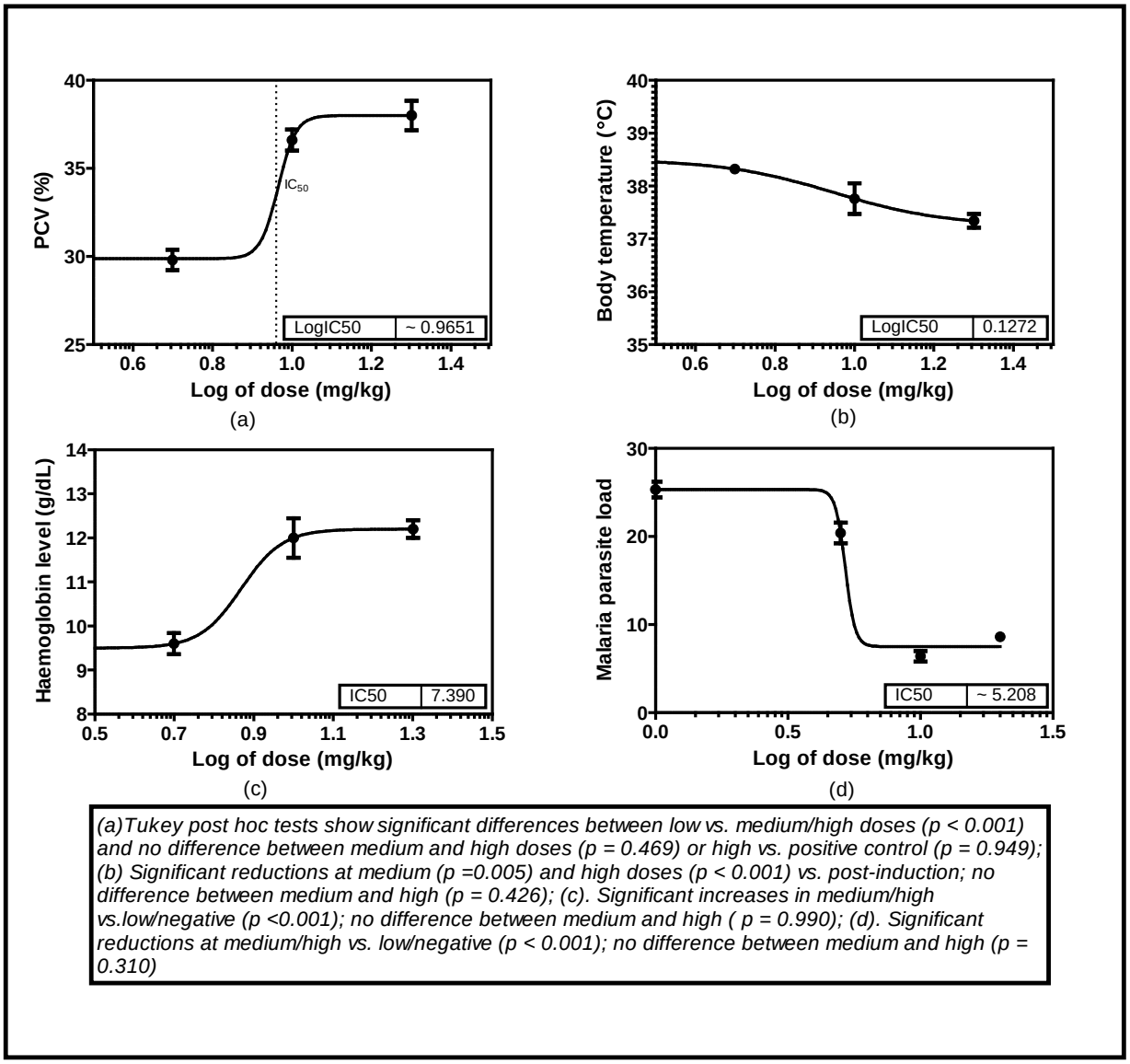

Figure 7 *Dose-response curves for biosynthesised silver nanoparticles in antimalarial treatment. Trend description for (e) Packed cell volume (f) Body temperature (g) Haemoglobin levels (h) Malaria parasite load*

4. Discussions

The green synthesis approach successfully yielded a highly stable and efficacious silver nanoparticle (GL-AgNP) composite, whose functional properties are inextricably linked to its unique structural signature: a metallic Ag^0 core passivated by a thick, natural biopolymer matrix (Figure 8a).

Structural Characterization and Validation of the Bio-Support Matrix

The successful formation of the GL-AgNPs was first confirmed by UV-Vis analysis, showing the characteristic Surface Plasmon Resonance (SPR) peak at 431 nm. The observed bathochromic shift (red shift) is a direct consequence of the high refractive index created by the surrounding organic biopolymer matrix, a structural feature characteristic of biosynthesis [14, 15]. This matrix was decisively identified by FTIR analysis, which confirmed the involvement of potent reducing agents (O-H groups) and essential stabilizing agents (Amide I/II bands from proteins), supporting a multi-group stabilization mechanism. Further confirming the composite nature, EDX showed a high percentage of silver (80.67%) alongside significant amounts of light elements like Carbon (7.00%), Nitrogen (2.16%), and Sulphur (1.15%), which are core constituents of the stabilizing biomolecules.

Particle size analysis (DLS) confirmed a small hydrodynamic diameter of 43.04 nm, ideal for nanomedicine applications [11]. The moderate polydispersity (PDI = 0.346) is acknowledged not as a limitation, but as a structural signature of the chemical heterogeneity inherent in using crude biological extracts[12]. This hydrodynamic size, when compared to the smaller core size definitively visualized by TEM (2.91 nm), accurately represents the thickness of the external organic solvation layer. The visible, thick organic layer in the TEM images, alongside the irregular bulk morphology observed in SEM, provides conclusive visual evidence of the robust Ag/biopolymer composite structure. The only resulting structural ambiguity, the definitive absence of the characteristic FCC metallic silver peaks in the XRD pattern, is directly attributed to the overwhelming presence of this thick, amorphous biopolymer shell masking the weak signal of the nano-crystalline core. This is depicted in Figure 8a. These findings are consistent with broader literature reviews that characterize the stabilization of nanoparticles via plant-derived secondary metabolites [16]. We propose that the organic-related peaks in the XRD should be viewed as a desirable marker for superior safety in biosynthesized metallic nanoparticles [17].

Safety, Efficacy, and Dual-Action Therapeutic Potential

The established structural passivation directly translated into an exceptionally favourable acute safety profile. The GL-AgNPs demonstrated no acute toxicity up to the maximum tested dose, placing the LD_{50} at > 5000 mg/kg—a testament to the protective function of the biopolymer matrix in minimizing the release of toxic Ag^+ [7, 8]. This high degree of safety provided a broad therapeutic index when contrasted with the excellent antimalarial efficacy observed *in vivo*.

The 4-day suppressive test compellingly demonstrated potent, dose-dependent efficacy against *Plasmodium berghei,* achieving a maximum suppression of 85.0% at a low therapeutic dose (20 mg/kg). Furthermore, a major finding was the clear evidence of an anti-anaemic effect: the GL-AgNPs significantly prevented the drop in PCV seen in the control group. This suggests a dual therapeutic mechanism: direct parasite killing (reducing iRBC destruction) and a nanoparticle-mediated protective effect, possibly stabilizing uninfected RBCs or modulating inflammation (Figure 4).

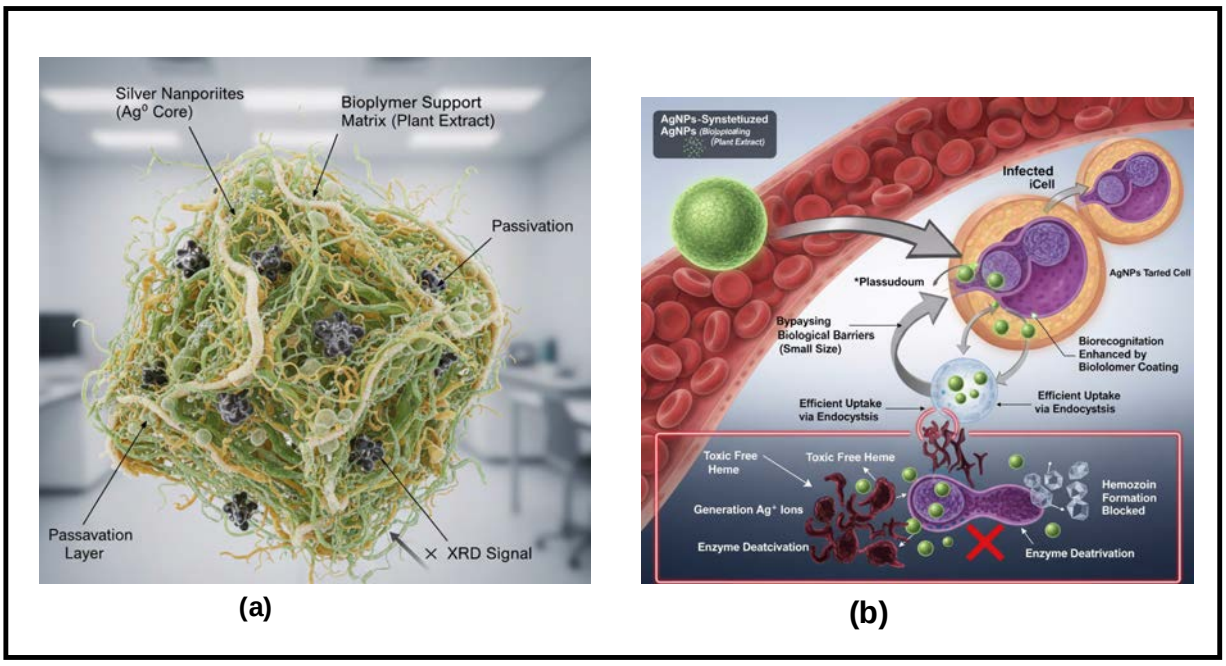

Figure 8 (a) Depiction of Green-synthesised silver nanoparticle Ag^0 cores embedded in a biopolymer passivation matrix (b) A proposed mechanism of action GL-AgNPs

Proposed Mechanistic Pathway

The potent antimalarial action of the GL-AgNPs is supported by a multifaceted, synergistic mechanism that takes advantage of the unique nanostructure of the material (Figure 8a) [18-20].

1. Enhanced Uptake and Targeting: The small size (43.04 nm) and the biorecognition properties of the biopolymer coating enhance affinity for infected red blood cell (iRBC) surfaces, promoting efficient endocytic uptake into the parasite's food vacuole.
2. Targeted Heme Disruption: Inside the acidic food vacuole, the Ag0 core or released Ag^+ ions interfere with the essential process of beta-haematin crystallization, leading to the accumulation of toxic free heme.
3. General Cytotoxicity: This targeted action is amplified by general cytotoxicity, where the GL-AgNPs generate Reactive Oxygen Species (ROS) and the released Ag^+ ions bind to and deactivate critical parasite enzymes (e.g., thioredoxin reductase via sulfhydryl groups), leading to metabolic collapse and parasite lysis.

Thus, the successful green synthesis yielded a structurally unique Ag/biopolymer composite whose superior safety and potent, multi-action antimalarial efficacy strongly validate it as a promising candidate for next-generation nanomedicine against drug-resistant malaria.

5. Conclusion

This work successfully demonstrated the eco-friendly, green synthesis of a highly functional silver nanoparticle (AgNP) composite, fully validating the relationship between its unique biostructure and superior biological performance. Rigorous characterization confirmed the formation of spherical, biopolymer-passivated AgNPs with an optimal hydrodynamic size of 43.04 nm. The collective spectroscopic and microscopic data—including the UV-Vis SPR red-shift at 431 nm, the DLS/TEM size discrepancy, the FTIR biocompound signatures, and the high C/N/S EDX content—all converged to establish the presence of a thick, protective organic capping layer. Crucially, this structurally confirmed passivation layer translated directly into an exceptionally favourable acute safety profile (LD_{50} > 5000 mg/kg), validating the hypothesis that the green synthesis route minimizes silver toxicity.

The *in vivo* efficacy demonstrated substantial suppression of *P. berghei* parasitemia, positioning these AgNPs as a promising therapeutic agent. Their antimalarial action is driven by a multifaceted mechanism: enhanced uptake into iRBCs via their nanoscale size and biopolymer coating, followed by targeted disruption of parasite heme detoxification and amplification through generalized oxidative stress. In summary, the GL-AgNPs represent a stable, highly biocompatible, and efficacious nanomedicine, offering a sustainable and cost-effective strategy for developing next-generation treatments to combat the critical challenge of drug-resistant malaria.

Acknowledgements

We extend our sincere gratitude to Professor Kenneth O. Okolo and Professor Daniel L. Ajaghaku, both of the Department of Pharmacology and Toxicology at the ESUT Pharmacy School, Agbani. Their invaluable guidance and expertise were instrumental in shaping the methodology used to study and establish the preliminary toxicity profile (LD_{50}) of GL-AgNPs. We also gratefully acknowledge the specialized technical support received during the biological evaluation of this work. We particularly thank Chief Raymond Okonkwo of the Department of Pharmacology and Toxicology at the ESUT Pharmacy School for his dedicated efforts in successfully carrying out the induction and treatment of parasitemia in the murine model. Our appreciation also extends to Ms. Love Ukamaka Onuoha of the Department of Clinical Pharmacy and Biopharmaceutics at the ESUT Pharmacy School for her meticulous work in handling the core analytical aspects, including the PCV, Haemoglobin (Hb), and Parasitemia determinations.

Author Contributions

Goodnews Onyedikachi Ikeh: Conceptualization, Methodology design, Funding acquisition, Synthesis of GL-AgNPs, Nanoparticle characterization, Writing—Original Draft Preparation. Nkoyo Imelda Nubila: Data Curation (Bioevaluation data), Formal analysis (Statistical analysis). Njideka Ifeoma Ani: Data Visualization (Generation of dose-response curves). Chidiebere Collins Igwe and Ogeh Emmanuel Chukwuebuka: Resources (Curated literature review materials. Amaka Barbara Ogbuagu and Rita Chiamaka Okpoto: Investigation (Assisted during the synthesis of GL-AgNPs). All authors read and approved the final manuscript.

References

[1] World Health Organization. World Malaria Report. Geneva: World Health Organization; 2023. Available from: https://www.who.int/teams/global-malaria-programme/malaria-reports/world-malaria-report-2023

[2] Ikeh GO, Ugwu PE, Okpoto RC, Njoku EA, Diovu CC, Adonu CC. Biogenic Synthesis and Comparative Assessment of the Antimicrobial Activities of Silver and Zinc Nanoparticles of Dialium Guineense Leaf Extract Against Human Pathogens. J Complement Altern Med Res. 2024;25(12):211-26. https://doi.org/10.9734/jocamr/2024/v25i12607

[3] Liu Z, Niu J, Niu C. Green synthesis of silver nanoparticles and their antimalarial activity. Int J Nanomedicine. 2019;14:4663-72. https://doi.org/10.2147/IJN.S209459

[4] Rai M, Ingle AP, Paralikar P, Gupta I, Medici S, Santos CA. Recent advances in use of silver nanoparticles as antimalarial agents. Int J Pharm. 2017;526(1-2):254-70. https://doi.org/10.1016/j.ijpharm.2017.04.042

[5] Gupta M, Seema K. Living Nano-factories: An Eco-friendly Approach Towards Medicine and Environment. In: Pal K, editor. Bio-manufactured Nanomaterials. Cham: Springer; 2021. p. 115-132. https://doi.org/10.1007/978-3-030-67223-2_6

[6] Shayo GM, Elimbinzi E, Shao GN. Preparation methods, applications, toxicity and mechanisms of silver nanoparticles as bactericidal agent and superiority of green synthesis method. Heliyon. 2024;10(17):e36539. https://doi.org/10.1016/j.heliyon.2024.e36539

[7] Alwhibi MS, Soliman DA, Awad MA, Alangery AB, Al Dehaish H, Alwasel YA. Green synthesis of silver nanoparticles: Characterization and its potential biomedical applications. Green Process Synth. 2021;10(1):412-20. https://doi.org/10.1515/gps-2021-0039

[8] Anum F, Jabeen K, Javad S, Iqbal S, Tahir A, Javed Z, et al. Green synthesized silver nanoparticles as potent antifungal agent against Aspergillus terreus Thom. J Nanomater. 2021;2021:2992335. https://doi.org/10.1155/2021/2992335

[9] Okorie NH, Ikeh GO, Adonu CC, Okorie CP, Omeh RC, Nwangwu AK. Precursor Chemistry and Antimicrobial Performance: A Green Synthesis Approach to the Zinc Oxide Nanoparticles. Asian J Appl Chem Res. 2025;16(2):116-40. https://doi.org/10.9734/ajacr/2025/v16i2333

[10] Organisation for Economic Co-operation and Development. OECD Guideline for the Testing of Chemicals: Acute Oral Toxicity - Fixed Dose Procedure. Paris: OECD Publishing; 2020. Available from: https://www.oecd.org/en/publications/test-no-420-acute-oral-toxicity-fixed-dose-procedure_9789264070943-en.html

[11] Salata OV. Applications of nanoparticles in biology and medicine. J Nanobiotechnology. 2004;2(1):3. https://doi.org/10.1186/1477-3155-2-3

[12] Kora AJ, Rastogi L. Enhancement of antibacterial activity of capped silver nanoparticles in combination with antibiotics, on model gram-negative and gram-positive bacteria. Bioinorg Chem Appl. 2013;2013:871097. https://doi.org/10.1155/2013/871097

[13] Jalab J, Abdelwahed W, Kitaz AM, Al-Kayali R. Green synthesis of silver nanoparticles using aqueous extract of Acacia cyanophylla and its antibacterial activity. Heliyon. 2021;7(9):e08033. https://doi.org/10.1016/j.heliyon.2021.e08033

[14] Joshi P, Pandey L, Patel A, Baksh Z, Singh P, Singh R. Green Synthesis and Characterization of Silver Nanoparticles Using Stachytarpheta indica. Int J Curr Microbiol Appl Sci. 2025;14(4):163-72. https://doi.org/10.20546/ijcmas.2025.1404.004

[15] Shahzadi S, Fatima S, ul ain Q, Shafiq Z, Janjua MRSA. A review on green synthesis of silver nanoparticles (SNPs) using plant extracts: a multifaceted approach in photocatalysis, environmental remediation, and biomedicine. RSC Adv. 2025;15(5):3858-903. https://doi.org/10.1039/D4RA07519F

[16] Vanlalveni C, Lallianrawna S, Biswas A, Selvaraj M, Changmai B, Rokhum SL. Green synthesis of silver nanoparticles using plant extracts and their antimicrobial activities: a review of recent literature. RSC Adv. 2021;11(5):2804-37. https://doi.org/10.1039/D0RA09941D

[17] Radulescu DM, Surdu VA, Ficai A, Ficai D, Grumezescu AM, Andronescu E. Green synthesis of metal and metal oxide nanoparticles: A review of the principles and biomedical applications. Int J Mol Sci. 2023;24(20):15397. https://doi.org/10.3390/ijms242015397

[18] Kamaraj C, Balasubramani G, Siva C, Raja M, Balasubramanian V, Raja RK, et al. Ag nanoparticles synthesized using β-caryophyllene isolated from Murraya koenigii: Antimalarial (Plasmodium falciparum 3D7) and anticancer activity. J Clust Sci. 2017;28(4):1667-84. https://doi.org/10.1007/s10876-017-1180-6

[19] Kojom Foko LP, Eya'ane Meva F, Eboumbou Moukoko CE, Ntoumba AA, Ngaha Njila MI, Belle Ebanda Kedi P, et al. A systematic review on anti-malarial drug discovery and antiplasmodial potential of green synthesis mediated metal nanoparticles. Malar J. 2019;18(1):337. https://doi.org/10.1186/s12936-019-2974-9

[20] Tiwari S, Kumar R, Devi S, Sharma P, Chaudhary NR, Negi S, et al. Biogenically synthesized green silver nanoparticles exhibit antimalarial activity. Discov Nano. 2024;19(1):136. https://doi.org/10.1186/s11671-024-04098-2